https://dx.doi.org/10.1016/j.envpol.2017.09.040

Speciation, mobilization, and bioaccessibility of arsenic in geogenic soil profile from Hong Kong

Jin-li Cui [a], Yan-ping Zhao [a], Jiang-shan Li [a], Jing-zi Beiyuan [a], Daniel C.W. Tsang [a], Chi-sun Poon [a], Ting-shan Chan [b], Wen-xiong Wang [c], Xiang-dong Li [a, *]

[a] *Department of Civil and Environmental Engineering, The Hong Kong Polytechnic University, Hung Hom, Kowloon, Hong Kong*

[b] *National Synchrotron Radiation Research Center, 101 Hsin-Ann Road, Hsinchu Science Park, Hsinchu 30076, Taiwan*

[c] *Division of Life Science, The Hong Kong University of Science and Technology (HKUST), Clearwater Bay, Kowloon, Hong Kong*

Corresponding author.

E-mail address: cexdli@polyu.edu.hk (X.-d. Li).

ABSTRACT

The behaviour of arsenic (As) from geogenic soil exposed to aerobic conditions is critical to predict the impact of As on the environment, which processes remain unresolved. The current study examined the depth profile of As in geologically derived subsoil cores from Hong Kong and investigated the mobilization, plant availability, and bioaccessibility of As in As-contaminated soil at different depths (0 – 45.8 m). Results indicated significant heterogeneity, with high levels of As in three layers of soil reaching up to 505 mg/kg at a depth of 5 m, 404 mg/kg at a depth of 15 m, and 1510 mg/kg at a depth of 27–32 m. Arsenic in porewater samples was <11.5 μg/L in the study site. X-ray absorption spectroscopy (XAS) indicated that main As species in soil was arsenate (As(V)), as adsorbed fraction to Fe oxides (41–69% on goethite and 0–8% on ferrihydrite) or the mineral form scorodite (30–57%). Sequential extraction procedure demonstrated that 0.5 ± 0.4% of As was exchangeable. Aerobic incubation experiments exhibited that a very small amount (0.14–0.48 mg/kg) of As was desorbed from the soil because of the stable As (V) complex structure on abundant Fe oxides (mainly goethite), where indigenous microbes partly (59 ± 18%) contributed to the release of As comparing with the sterilized control. Furthermore, no As toxicity in the soil was observed with the growth of ryegrass. The bioaccessibility of As was <27% in the surface soil using simplified bioaccessibility extraction test. Our systematic evaluation indicated that As in the geogenic soil profile from Hong Kong is relatively stable exposing to aerobic environment. Nevertheless, children and workers should avoid incidental contact with excavated soil, because high concentration of As was present in the digestive solution (<0.1–268 μg/L).

INTRODUCTION

Arsenic (As) contamination has been widely reported in various environmental matrices, including groundwater (Fendorf et al., 2010; Guo et al., 2014; Selim Reza et al., 2010), surface water (Smedley and Kinniburgh, 2002), and soil/sediment (Johnston et al., 2015; Kim et al., 2014). Arsenic contamination of groundwater systems could be caused by Fe (hydr)oxides reductive process induced by microbe or water table change in aquifer-soil- sediments system under anoxic conditions (Fendorf et al., 2010; Smedley and Kinniburgh, 2002), or by the oxidizing process of As-containing sulphide compounds (e.g., orpiment) when exposed to aerobic conditions (Polizzotto et al., 2005).

Recent studies have found high concentrations of As in groundwater in the Pearl River Delta (PRD), with As concentration reaching up to 176 μg/L (Liu et al., 2014; Wang et al., 2012). These high concentrations of As have been caused by microbial reductive process of Fe oxides under reducing conditions (negative Eh, e.g., -126 eV, and high DOC, e.g., 35.8 mg/L) (Wang et al., 2012). The mineral pyrite (FeS_2) found in sediment of the PRD (Wang et al., 2012) and another similar mineral mackinawite (tetragonal FeS) formed during floodplain soil incubation (Burton et al., 2014) play a role in immobilizing As because the iron sulfide compounds can adsorb As under anaerobic conditions and slightly alkaline pH (Niazi and Burton, 2016).

A recent soil survey in the Northeast New Territories of Hong Kong showed high concentrations of As up to 23,400 mg/kg in the soil (HK CEDD, 2015). These high levels in the soil may pose a severe risk to the environment. The biogeochemical behaviour of geogenic As in soil exposed to oxygen and the environmental matrix during construction work and soil excavation for urban development remains unclear.

Once soil is excavated for urban development, geogenic As may be released because of the competition to adsorb on Fe oxide sites from various inorganic chemicals, organic compounds,

and com- plex environmental matrices, such as rainwater and plant vegetation (Bergqvist et al., 2014; Cui et al., 2015b; Liu et al., 2016; Youngran et al., 2007). Under high redox levels of 200–500 mV exposed to oxygen, the amount of As released from contaminated soil was low, with arsenate (As(V)) as the major aqueous species (65–98%) (Masscheleyn et al., 1991). When carbon sources including low-molecular-weight organic acids (LMWOAs) such as citrate are present, As(V) can be effectively reduced to arsenite (As(III)) by aerobic As-resistant bacteria harbouring the arsC gene (Corsini et al., 2011; Tian et al., 2015). The reduction from As(V) to As(III) possibly results in high aqueous As because As(III) has a lower affinity than As(V) to Fe (hydr)oxides (Pierce and Moore, 1982; Smedley and Kinniburgh, 2002). Furthermore, As availability can be incresded in As-contaminated soil with vegetation because the root organic exudates facilitate the release of As, which may retard plant growth due to the toxicity of As (Bergqvist et al., 2014; Liu et al., 2016). Excavated soil particles containing As may be incidentally ingested in the human body during construction work, and should be evaluated for As bioaccessibility. Recently, various kinds of polluted soil from mining and smelting sites (Corsini et al., 2011; Kim et al., 2014; Li et al., 2014; Meunier et al., 2010), cattle dip sites using As-based pesticides (Burton et al., 2014; Juhasz et al., 2007; Niazi et al., 2011), and e-waste sites (Cui et al., 2017) have been studied; however, further evaluation is required of the environmental behaviour and mechanism for the release of As from underground geogenic soil.

The above discussed mobilization, plant availability, and bio- accessibility of As is largely determined by As chemical speciation in soil (Foster and Kim, 2014; Kim et al., 2014; Niazi et al., 2011). The general chemical fractions of As in soil can be characterized using a sequential extraction procedure (SEP) (Wenzel et al., 2001) to evaluate the exchangeable and adsorbed species at the macroscopic level. Furthermore, synchrotron-based X-ray absorption spectros- copy

(XAS) was also used to in situ characterize the molecular speciation of As in soils, including oxidation states, neighbouring atoms, and local distances (Gr€afe et al., 2014; Kelly et al., 2008). The objectives of this study were: (1) to evaluate the potential release and transformation of As; and (2) to elucidate the underlying mechanisms controlling the biogeochemistry of the As in the geogenic soil under aerobic environmental conditions once the soil has been excavated from the subsurface.

MATERIALS AND METHODS

Soil Collection

A total of 198 soil samples from 16 soil cores (with a maximum depth at 45.8 m below the surface) were obtained from the Northeast New Territories, Hong Kong, as has been previously re- ported (HK CEDD, 2015; Li et al., 2017). Hong Kong has humid subtropical weather with an annual average temperature of 23.3°C and precipitation of 2398.5 mm (Hong Kong Observatory, 2011). The collected soil columns were wrapped using cling film and capped on site, transported to a laboratory, and dismantled in the laboratory as quickly as possible. The sectioned soil samples were passed through a 2-mm sieve, dried at 60°C until the weights were consistent, ground and mixed homogeneously, and stored in the dark before being analysed. Parts of the soil columns were trans- ported to the laboratory on ice, and stored at 4°C until incubation experiments and a spectroscopic analysis could be conducted.

The air-dried samples from different soil columns were divided into three groups according to the total As concentrations of the risk-based remediation goals, including a low level of 21.8 mg-As/kg in urban/rural residential soil, a medium level of 73.5 mg-As/kg in public park soil, and a high

level of 196 mg-As/kg in industrial soil (HK EPD, 2007). After homogeneous blending, the soil samples were ground and used in further experiments. The average As concentrations in the three composite soil samples (dry weight) were 55.8 mg/kg (low level), 101 mg/kg (medium level), and 347 mg/kg (high level), respectively (Beiyuan et al., 2017).

Arsenic mobility and bioavailability in soil

The mobility of the As in soil was measured by aerobic incu- bation experiments exposed to the environmental matrix at 25°C in a shaking incubator. The representative soil samples from a depth of 18.9–19.6 m from the collected core-3 (Li et al., 2017) containing 1480 mg-As/kg and 32,100 mg-Fe/kg was used for incubation. The incubation experiments and sampling procedure were performed in triplicate using aseptic techniques. The soil (3 g), which had been stored at °C, was mixed with solutions (40 mL) containing inorganic salts (10 mM KCl, 10 mM $NaNO_3$, or 10 mM Na_2SO_4), organic salts (10 mM sodium acetate or 1 mM sodium salicylate), or synthetic rainwater (Table S1) - conditions that are commonly found in the natural aqueous/soil matrix (Burton et al., 2014; Li and Xu, 2007). Formaldehyde at a concentration of 0.04% was added to the control experiments to inhibit the microbial activities in the soil (Corsini et al., 2011). Because oxygen was being consumed at an unexpected rate, the bottles, which were placed on a sterile bench, were opened to the air every three days. During sampling on 7, 14, and 28 days, suspension samples were collected after the bottles were shaken until the suspension were homogenous, monitored using a pH meter (Model 225 m, Denver Instrument), centrifuged, and filtrated through a 0.2 μm membrane filter. The TOC in the filtrated solution was detected using TOC analyser (SHIMADZU, model: ASI-5000 A). After the aqueous samples were collected, the final centrifuged soil samples

were washed three times using a fresh corresponding solution. The remaining solids were freeze-dried under a vacuum for further characterization.

To determine As plant availability, the three kinds of mixed soil samples with different As contamination levels mentioned above were used in the pot experiments. Twelve representative surface soil (<250 mm, 0–0.50 m) samples selected on the basis of the spatial distribution of the sampling cores in the study site (HK CEDD, 2015), which are easily inhaled and ingested by humans, especially children (Juhasz et al., 2007), were evaluated using a simplified bioaccessibility extraction test (SBET) extraction. More detailed information about the pot experiments and the SBET extraction can be found in the supplementary data.

Sample analysis

The dried soil and plant samples were digested with concentrated HNO_3 and $HClO_4$ on a hot plate (Bergqvist et al., 2014; Li et al., 2004) with the NIST SRM 2711a as a reference for recovery rates for As (105 ± 7%) and Fe (88 ± 3%). Total As and Fe in all of the samples were analysed using ICP-MS (Agilent, 7700 Series) or ICP- OES (Agilent, 700 Series), depending on the concentration. The species of As(III) and As(V) were checked using high-performance liquid chromatography hydride generation atomic fluorescence spectrometry (HPLC-HG-AFS) (Zhang et al., 2013).

Five operationally defined chemical fractions of As in the surface layers from 0 to 1.50 m from selected cores were analysed using a traditional modified SEP method (Wenzel et al., 2001). Details of the process are given in the supplementary data. The As phases were operationally defined into the following five fractions: non-specifically-bound (F1), specifically-bound (F2), amorphous hydrous oxide-bound (F3), crystalline hydrous oxide-bound (F4), and the residual (F5).

The solid phase speciation of As and Fe in selected soil samples was done using As K-edge (11,867 eV) XAS spectra at beamline BL01C1 and Fe K-edge (7112 eV) XAS spectra at beamline BL16A1 at the National Synchrotron Radiation Research Center in Taiwan. Specifically, As K-edge X-ray absorption near edge structure (XANES) was employed to elucidate the solid phase species of As (including As(III), As(V), or As-S like species) in the soil. Arsenic K- edge extended X-ray absorption fine structure (EXAFS) was used to characterize the complex structure of As in the soil samples. Arsenic references included Na2HAsO4 · 7H2O, $NaAsO_2$, orpiment (As_2S_3), realgar (AsS), arsenoypyrite (FeAsS), As(V/III) adsorbed species on goethite (Gt) or ferrihydrite (Fh). Ten Fe-bearing reference compounds were included: ferrihydrite, goethite, magnetite (Fe_3O_4), hematite, FeS_2, scorodite, FeAsS, and $FeSO_4$. More experimental and analytical details can be found in the supplementary data.

RESULTS AND DISCUSSION

Arsenic distribution in soil cores at different depths

The depth profile patterns of As and Fe in the soil cores are shown in Fig. 1. The results indicated that As concentration (2.3–1510 mg/kg) varied greatly in different soil cores and across depths, which is consistent with our previous results showing much heterogeneous distribution with concentrations ranging from 9.57 to 1985 mg/kg (Li et al., 2017). In general, the observed As values for the surface soil layer (0–0.50 m) ranged from 25.0 to 396 mg/kg, with a median concentration of 68.7 mg/kg.

With regard to the depth profiles, As levels were very heterogeneous in the cores. In particular, different patterns were observed between “offsite” and “offsite a”, which were only five metres

apart. Elevated levels of As were observed in three layers of soil at approximately 5 m (where the highest value was 506 mg/kg), 15 m (highest value of 404 mg/kg), and 27–32 m (highest value of 1510 mg/kg) below the surface, similar to a previous report (Li et al., 2017). These As concentrations are much higher than those in surface soil in Hong Kong (16.5 ± 4.5 mg-As/kg) (Chen et al., 1997), in background soil in Guangdong province (10.4 mg-As/kg) (Zhang et al., 2006), and in the earth's mantle and crust (0.05–5.1 mg-As/ kg) (Henke, 2009). A previous study conducted in the PRD area (Guangzhou, Foshan, and Zhongshan) indicated relatively low concentrations of As in the sediment cores with depth from 3 to 39.4 m, ranging from 5 to 40 mg/kg, with the highest concentration being found at a depth of ~5 m below the surface (Wang and Jiao, 2014; Wang et al., 2012).

The As depth distribution in some cores may demonstrate different profiles from those in the three recognized layers, such as the ~8 m depth layer in column 01a or the ~23 m depth layer in the column offsite. The distribution of trace elements in soil cores should be determined by the parent soil matrix and by the history of a site development. The historical use of the land in the study areas was reviewed with the aid of the historical aerial photo- graphs. No direct association was shown between human activities and the high levels of As that were detected (HK CEDD, 2015), especially at depths of up to ~20 m below the surface. Therefore, anthropogenic activities seem not the source of the As contamination in the study site, which should originate from geogenic formation.

In addition, high concentrations of Fe along the soil profiles were observed in the collected cores, ranging from 907 to 26,700 mg/kg, with a median value of 10,800 mg/kg (Fig. 1). The ratios of As/Fe (mg/g) in the soil varied from 0.3 to 141 (14.4 ± 16.9, with a median value of 8.2), much higher than the values (0.3–1.1) of the sediment where Fe oxides effectively scavenge the

208 dissolved As from aquifers (Wang et al., 2012). Other studies also reported that As was principally
209 retained on Fe oxides with smaller As/Fe ratios (mg/kg) of 1.0–3.0 in the Red River Delta (Eiche
210 et al., 2010) and 3.2 x 10^{-6} to 0.12 in the Hetao Basin (Deng et al., 2011). Although Fe oxides in
211 soil may acts as a natural carrier of As because of their high adsorption capacity (Datta et al., 2009;
212 van Geen et al., 2006), the much high content of As in the collected soil still merits further
213 evaluation of its biogeochemical behaviour.

214

215 **Sequential extraction procedure and X-ray absorption spectroscopy for speciation of As in**
216 **soils**

217 A sequential extraction scheme may indicate various geochemical pools of As on the surface
218 (labile fraction) of soils or the process of the incorporation (non-labile fraction) of As into the
219 minerals of the soil, which can partly elucidate the biogeochemistry of As in soils (Datta et al.,
220 2009). The sequential extraction results (Fig. 2) indicated that As in the soils are primarily
221 associated with crystalline Fe/Mn/Al oxides (F4), with 56.4 ± 15.5% (median value of 54.4%) as
222 the largest fraction, and then with the residual fraction (F5), with 20.6 ± 11.9% (median value of
223 16.0%), which is consistent with our previous samples in the near site (Li et al., 2017). The As
224 incorporated in F4 and F5 should be either co-precipitated into or adsorbed on the Fe/Mn/Al oxides
225 in the soil matrix (Kim et al., 2014; Root et al., 2009; Wenzel et al., 2001). The As fractions in F4
226 plus F5 represent the non-labile fractions and are not easily mobilized, because the host minerals
227 are relatively resistant to the redox change and dissolution (Haque et al., 2008). Previous studies
228 have also indicated that high concentrations of As in the sequential factions F4 plus F5 results in
229 low (bio)available As to the solution (Ngo et al., 2016; Niazi et al., 2011).

The non-specifically bound fraction (F1) of As was 0.5 ± 0.4%, representing the lowest fraction of the total As. Arsenic fraction in F1 represents the easily labile As, which should be critical in determining As levels in the aquifer (Kim et al., 2014; Wenzel et al., 2001). The specifically bound fraction (F2) also accounts for relatively low proportions (9.6 ± 4.6%) in soil cores, whereas amorphous hydrous oxide-bound (F3), which made up 12.9 ± 8.8% of the total As, is associated with amorphous Fe hydroxides. Arsenic in fractions of F1, F2, and F3 may be released into aquifers under the competitive effect of co-existing ions, high pH, or the fluctuation of the redox potential (Cui et al., 2015b; Fendorf et al., 2010; Smedley and Kinniburgh, 2002; Youngran et al., 2007).

Besides the sequential extraction fraction, the As oxidation state is also important for As mobilization process because the reduced As(III) has a lower affinity to the surfaces of soil minerals and a higher mobility than As(V) (Pierce and Moore, 1982). Therefore, As oxidation speciation in the selected soil samples was further evaluated using XANES spectroscopy.

The linear combination fitting (LCF) analysis of the first derivative of XANES spectra indicated that As(V) was predominant (>98%) in the detected soil samples (Fig. 3, Fig. S2, and Table S2), with low content of As(III) or sulfide bound species (amounting to 1–3% combined). Other selected soil samples identified using XANES and XPS analysis also showed that As(V) is a major species, exceeding 90% of total concentrations (Beiyuan et al., 2017). Of the As(V) species, 41–69% were associated with adsorbed species (41e69% as goethite adsorbed fraction and 0–8% as ferrihydrite adsorbed fraction) and 30e57% as scorodite mineral, based on the XANES analysis (Fig. S2). These are relatively stable species (Kim et al., 2014; Meunier et al., 2010). The presence of these two As(V) associated species coincided with the large non-labile fraction of F4 plus F5 in soils, as detected in the sequential extraction analysis.

The dominance of As(V) in the soil samples may reflect the oxidizing aquifer in the study site. In one study from Bangladesh, As was mainly As(V) (e.g. 78–90% in As(V)) and As(III), with no As-S in subsurface sediments (1–3 m depth) (Datta et al., 2009). In sediment collected from an oxidized zone (Root et al., 2009), contents of As(V) exceeding 98.7% were observed, which is consistent with our study. Much lower percentages of sulphide bound As (<2%, Table S2) was observed in the analysed samples. The relatively stable As(V) rather than the As(III) in the oxidizing matrix, together with the abundant Fe oxides, could substantially limit the mobilization of As from soil (Smedley and Kinniburgh, 2002; Watts et al., 2014). During this study, four porewater samples were available, showing less than 11.5 mg/L As coexisting with 5.5–27.2 mg/L Fe (Table S4). The low As concentration in the soil porewater is consistent with the orange colour of our soil samples, which often indicates the presence of abundant amounts of Fe(III) oxides and low concentrations of organic matter (Fendorf et al., 2010; van Geen et al., 2006).

Previous studies have often suggested that As in sediment is primarily in As(III) rather than As(V). For example, 55% of As(III) and 17% of orpiment-like species with 28% in As(V) were found in sediments in Bangladesh at a depth of 30 m (Polizzotto et al., 2005). Abundant As-sulphide species (~30–80%) were also found in organically rich layers in Nepal (Johnston et al., 2015), where, under relatively stable reducing conditions, authigenic FeS2 often plays a critical role in controlling aqueous As. In the PRD, a study was conducted using XANES to investigate the As speciation in soil (Wang et al., 2013), where As(V) was found at a percentage of 23% at a depth of 17.4 m and As(V) at 46% was found at 18.5 m, while other species were As(III) (23–36%) and arsenopyrite (30–41%). The co- existence of the various oxidation states of As can be caused by the properties of the soil/sediment and by a complex aquifer system, where the As is subjected to fluctuating redox conditions (Johnston et al., 2015; Smedley and Kinniburgh, 2002).

275 The analysis suggested that under undisturbed conditions the high As content in soil may not be
276 easily desorbed or released due to the strong ability of As to bind with Fe oxides, including ferri-
277 hydrite, goethite, and hematite (Datta et al., 2009; Root et al., 2009; Selim Reza et al., 2010),
278 especially in the case of oxic aquifers where low As concentrations are often found in groundwater
279 (Guo et al., 2014; Masscheleyn et al., 1991; Root et al., 2009). Although the As in the soil seems
280 stable, the biogeochemistry of the As may be influenced by external nutrients, including nitrate,
281 sulphate, and some organic chemicals in the aquifer caused by recent human activities.

282

283 **Arsenic mobility and speciation change during soil incubation**

284 During the soil incubation, 10.5e36.0 μg-As/L was observed in all of the suspensions at 8 days,
285 with the exception of the salicylate- treated solution, which contained 111 μg/L As (Fig. 4-I),
286 exceeding the WHO drinking water standard of 10 μg/L. The common anions, including chloride,
287 nitrate, sulphate, and acetate, often compete with the mobilizable As fractions for mineral surface
288 sites in the soil, showing no obvious dissolution effect on Fe oxides (Mohapatra et al., 2005;
289 Youngran et al., 2007). As the days went by in the 28- day sampling period, the initial As that had
290 been released in the first few days was re-adsorbed on the soil, leaving 5.0 - 24.1 μg/L As in the
291 final suspension. The total amount of As desorbed in 28 days 0.14 - 0.48 mg/kg, 0.01 - 0.03% of
292 the total As in the soil) was slightly less than the exchangeable fraction (1.63 mg/kg) of the original
293 soil. Aqueous Fe was also observed in the range 86.6 - 219 μg/L for the treatment by the common
294 anions (Fig. 4-III). In this study, the markedly lower desorption (leaching) of As from the soil can
295 largely be attributed to the less available As characterized by the SEP and XANES. In the
296 suspension, As(V) was the primary species in all of the incubated suspensions, with only 0.6 - 1.3
297 μg/L of As(III) in the salicylate-treated samples. Under an oxic matrix, aqueous As(V) displays a

stronger affinity than the common anions to adsorb on Fe oxides (Cui et al., 2015b; Masscheleyn et al., 1991; Youngran et al., 2007). The predominance of As(V) in the soil also alleviated the mobilization of As from the soil, especially under slightly acidic pH conditions (4.62 - 6.41 in the treated incubation and 4.31 - 5.57 in the sterilized control, as shown in Fig. S4) (Masscheleyn et al., 1991). The few mg/L of As remaining in the suspension at 28 days were at equilibrium between the suspension matrix and the solid surface. Of these, 5.3 ± 2.5 μg/L of As in the KCl treatment was at approximately a similar level of magnitude as the As detected in the collected porewater samples (less than 11.5 μg/L, Table S4).

The addition of salicylate significantly increased the desorption of As (1.48 mg/kg) from the soil in comparison with the common anions, i.e., leaving 102e111 mg/L in the suspension during the incubation period (8 - 28 days, Fig. 4-I). A longer incubation time brought little change in the As concentrations in the salicylate suspension. A high concentration of 680 μg/L Fe was observed in the suspension (Fig. 4-III), which was probably caused by salicylate combining with the Fe oxides in the soil (Li and Xu, 2007), which would result in the release of As into the aquifer, as identified by the positive association of aqueous Fe and As (Figs. S5eI). Furthermore, salicylate can strongly chelate with aqueous Fe and form relatively stable complexes (Alvarez-Ros et al., 2000), which to some extent would inhibit the precipitation of fresh Fe oxides (Haas and Dichristina, 2002).

Iron species in the original and treated soil samples were analysed using Fe K-edge XANES (Fig. S3 and Table S3). The results indicated that the original soil was primarily composed of goethite (65%), with a few other oxides including ferrihydrite (18%), hematite (5%), and scorodite (11%). The scorodite observed from the Fe XANES analysis is consistent with the discovery of scorodite from the As XANES analysis. After treatment, although goethite (59e70%) still dominated in the soils, the amount of ferrihydrite had increased slightly to 27% after incubation, compared with the

original fraction (18%). A slightly higher percentage of ferrihydrite was found in the microbial incubation in comparison with the sterilized control. The slightly higher level of ferrihydrite in the soil after incubation indicated that the Fe ions that had initially (microbially or chemically) been released from the soil had been re- adsorbed on the soil, forming the amorphous ferrihydrite. These processes facilitated the re-adsorption of the aqueous As to the soil, consistent with the slightly increasing amount of the adsorbed As(V) on ferrihydrite from 8% in the original soil to 8 - 25% after soil incubation (Table S2).

The addition of LMWOAs or nutrients to soil might facilitate the culture of the indigenous microbe. Previous studies also observed that the microbial reduction of Fe(III) (hydr)oxides can occur in soil during aerobic incubation using LMWOAs or soil organic matter as a carbon source, which may release the Fe-bearing As (Bongoua-Devisme et al., 2013; Kuhn et al., 2013). Nevertheless, a previous study indicated that the indigenous microbe in the sediment at a depth of 30 m resulted in less As desorption in anaerobic incubation than was observed in the abiotic control (Polizzotto et al., 2006). The varying significance of the indigenous microbe on As desorption/release from the sediment may be influenced by their abundance, cultivability, and soil/suspension chemistry.

In the sterilized soil, the concentration of aqueous As decreased significantly by 59 ± 18% in comparison with the respective incubation without sterilization over the experimental period (28 days) (Fig. 4-I&II). The results of the comparison suggest that the release of As from the soil is partly promoted by the indigenous microbe, and not only by the chemical leaching process. The release of Fe also decreased after sterilization during the first 15-day incubation (62 ± 26%, Fig. 4-III&IV). After 28 days, aqueous Fe was present in the suspension at the much lower concentration of <20 μg/L for all treatments with no significant association with aqueous As (Fig. S5- II), with the exception of the treatment with strong chelate salic- ylate (0.23 - 0.29 mg/L). The

general depletion of Fe in the sus- pension was likely caused by the rapid precipitation of Fe ions into Fe oxides in an aerobic circumneutral environment (Cui et al., 2015a; Kuhn et al., 2014).

Arsenic oxidation states and molecular structures in the soil during incubation should provide important information for elucidating the biogeochemical behaviour of As. The XANES anal- ysis indicated that there was still a major fraction (95 - 100%, Table S2) of As(V) in the incubated soil (Fig. 5-I). Arsenite in the incubated soil (ND - 5%, Table S2) slightly increased in comparison with the level in the original soil sample (1%). The increase of As(III) in the soil can be attributed to some microbial reductive reactions, although the percentage of As(III) was around the detection limit of 5 - 10% using XANES LCF analysis (Foster and Kim, 2014). On some occasions during oxic incubation, the Fe oxide in the soil can be aerobically reduced by microbes (Kuhn et al., 2013), and the associated As (primarily in As(V)) would be released into the suspension. Thereafter, the aqueous As(V) might be aerobically reduced to As(III) by some microbial species containing the arsC gene, including the Bacillus cereus strain (Corsini et al., 2011), Pantoea sp. IMH (Tian et al., 2015), and strains of Bacillus sp. M17-15 and Pseudomonas sp. M17-1 (Guo et al., 2015). Only a few μg/L of As(III) were found in the aqueous solution, possibly because As(III) is readily oxidized in aerobic circumneutral conditions (Smedley and Kinniburgh, 2002). During the 28-day incubation period, the aqueous As(III) and As(V) were re-adsorbed on the Fe oxides in the sediment (Fig. 4). The re-adsorption of aqueous As(III) onto the soil should contribute to an increase in solid As(III) (Tian et al., 2015), while the possible formation of secondary Fe minerals such as ferrihydrite (Fig. S3 and Table S3) under oxidized systems would also sequester As (Tufano and Fendorf, 2008). Nevertheless, the ability of aerobic microbes in the soil to reduce As(V) to As(III) merits future investigation.

The molecular structure of the As complex in the soil samples was further characterized using As K-edge EXAFS (Fig. 5-II&III and Table 1). The EXAFS analysis of the original soil sample showed that the first and strongest peak in the FT curve was contributed by four oxygen atoms at 1.67 Å. After incubation, the first peak was also fitted with oxygen, as no sulphide-bound species (Table S2) were observed from the LCF analysis of XANES. The fitting results suggested that 4.22 ± 0.20 oxygen atoms at 1.69 ± 0.01 Å contributed to the first strong peaks for all of the soil samples (Table 1). The fitting results of the first peaks showed little influence from the AsO3 structure, in which As was coordinated with 2.8 - 3.2 oxygen atoms at 1.76 - 1.78 Å (Ona-Nguema et al., 2005; Watts et al., 2014). The number and distance of the coordinations further demonstrated the presence of the AsO4 tetrahedral structure (Cui et al., 2015b; Jing et al., 2012; Sherman and Randall, 2003) in all of the incubated samples, confirming the LCF results from XANES. Twelve As- O-O-As triangular multiple scattering (MS) paths were implemented in the fit with distances of 3.05 ± 0.01 Å, in accordance with a previous study (Chen et al., 2009).

The second peaks of the incubated soils were fitted with 2.31 ± 0.46 Fe atoms at an inter-atomic distance of 3.22 ± 0.02 Å (Table 1). The fitted As-Fe distances in the soil samples were similar to the As-Fe distance (3.27 Å) for the adsorbed As(V) on goethite and a little shorter than that (3.32 Å) for scorodite, which is reasonable, as the primary species in the soil is the As(V) adsorbed species on goethite. These fitted inter-atomic distances were similar to those for a previously reported bidentate binuclear structure on goethite, at 3.23 - 3.24 Å (Fendorf et al., 1997), 3.27 - 3.28 Å (Jiang et al., 2013), and 3.30 Å (Sherman and Randall, 2003). The As-Fe distances were much shorter than the mono- dentate As-Fe distance of 3.67 Å (Sherman and Randall, 2003). Thus, the geogenic As primarily formed a bidentate binuclear inner- sphere complex on the Fe oxides in the sediment. No obvious difference was shown from the fitting results for the series of incubation

389 samples because the inner-sphere complex structure of As(V) is relatively stable and generally not
390 influenced by these inorganic and organic nutrients (Jing et al., 2012; Watts et al., 2014). The inter-
391 sphere adsorption complex is thermodynamically more stable (Sherman and Randall, 2003; Watts
392 et al., 2014), and limits the release of As into the aquifer, a process that alleviates the potential
393 human risk from As-contaminated soil.

394

395 **Arsenic availability under ryegrass vegetation**

396 When excavated soil is piled up or backfilled on the surface of the ground, plants, including grass,
397 often grow in the soil. The immobile As in soil may be dissolved in soil porewater possibly
398 facilitated by plant exudates, including various organic acids (Bergqvist et al., 2014; Liu et al.,
399 2016). Thus, the plant bioavailable fraction of As was studied by cultivating perennial ryegrass
400 using the three mixed soil samples with different concentrations of As.

401 After ryegrass was harvested, analytical results (Table S5) showed that the As concentration in the
402 shoots that were grown in soil with a low level of As was 1.08 ± 0.05 mg/kg. Arsenic
403 concentrations increased to 2.31 ± 0.64 mg/kg and 4.14 ± 0.35 mg/ kg when the shoots were
404 exposed to soils with medium and high levels of As, respectively. Similarly, the As content in the
405 roots also increased from 16.1 ± 3.2 mg/kg to 96.1 ± 18.9 mg/kg as the con- centration of As in
406 the soil increased (Table S5). The accumulation of As in the ryegrass was generally within the
407 range reported for non-hyperaccumulators, i.e., 0.31 - 150 mg/kg (Martinez-Lopez et al., 2014) or
408 1.2 - 95 mg/kg (Raab et al., 2007) in the roots, and 0.21 - 83.4 mg/kg (Martinez-Lopez et al., 2014)
409 or 0.1 - 5.2 mg/kg (Raab et al., 2007) in the shoots. The amount of As absorbed by a plant is usually
410 determined by the exchangeable (F1) and the specifically-bound fraction (F2) in the soil (Niazi et

411 al., 2011). The As amounts of F1 and F2 increased from 5.1 mg/kg, to 10.7 mg/kg, and to 30.4
412 mg/kg in the low, medium, and high As-bearing soils, respectively, which may have contributed
413 to the uptake of As by the plants. During the vegetation experiment, the ryegrass grew well in the
414 soil (Fig. S6), with no significant differences in biomass under the three levels of As (Table S5),
415 suggesting that the As-bearing soil had significant non-toxic effect on plant culture.

416

417 **Arsenic bioaccessibility as determined by a simplified bioaccessibility extraction test (SBET)**
418 **for human risk assessments**

419 Excavated As-bearing soil may pose a potential risk to human health in cases of incidental
420 ingestion, so the relative bio- accessibility of As was evaluated using the SBET assay (Juhasz et
421 al., 2007, 2009). The SBET results showed <0.1 - 268 μg/L in the extract, i.e., < 27% (9.5 ± 10.5%)
422 of As in the surface soil was bioaccessible (Table S8). The results indicated that a large proportion
423 of the total As in the surface soil was not available for assimilation in the gastrointestinal tract
424 following incidental soil ingestion. The bio- accessibility of As in the soil was relatively low in
425 comparison with published studies, such as 5.7 - 46.3% in surface soil (Das et al., 2013), 5 - 36%
426 in mine contaminated soils (Juhasz et al., 2007), and 6 - 89% in railway corridor soil (Juhasz et al.,
427 2007). Yet, it was slightly higher than the As bioaccessibility in smelter and mine contaminated
428 soil (0.9 - 11.1%), where the As was mostly associated with amorphous and crystalline iron oxides,
429 including scorodite (Kim et al., 2014).

430 The bioaccessibility of As in soil depends on the physical- chemical properties of the soil. An
431 analysis of the SBET extracts suggests that As bioaccessibility was positively associated with the
432 concentration of extracted Fe (Fig. S7), suggesting that the dissolution of Fe may contribute to the

release of As from the soil. An extractant solution with a low pH can dissolve the amorphous Fe to some extent, and possibly release Fe and the associated As. A paradoxical result with little association between SBET As bio- accessibility and Fe amounts was found in the soil in a previous study (Li et al., 2014). Iron oxides or the possible precipitated secondary mineral on the surface of the soil may adsorb the aqueous As in the gastrointestinal tract, and subsequently decrease the concentration of As in the suspension (Juhasz et al., 2009; Li et al., 2014).

Therefore, the much lower bioaccessibility of As in the tested soil samples should mainly be attributed to the stable As species associated with the abundant amorphous and crystalline Fe oxides (usually with 1 - 10% of the bioaccessibility of this fraction), especially in the form of scorodite (Kim et al., 2014; Meunier et al., 2010). Nevertheless, children and workers should beware of incidental ingestion when subsurface soil is excavated during construction work because of the existence of high levels of As with <0.1 - 268 μg/L (with a medium value of 30.0 μg/L, Table S6) in the digestive solution.

CONCLUSION

Our study indicates that heterogeneous depth profiles of As in soil cores from Hong Kong, reaching 1509 mg-As/kg, but only <0.1 - 11.5 μg/L for aqueous As was found in the porewater. XAS characterization indicated that As(V) (>98%) predominates in the soil, and is stably adsorbed/coprecipitated on abundant Fe oxides or formed crystalline scorodite via a bidentate binuclear structure, with a very minor fraction in exchangeable fractions, as determined from the SEP results, which should limit the release of As into water. The stable adsorption complex and strong binding ability of As on the Fe oxides was demonstrated by a very small amount of As that

was desorbed from the soil in the aerobic incubation experiments, although, apart from the chemical leaching process, the indigenous microbe partly (59 ± 18%) contributed to the release of As. Nevertheless, the bioaccessibility of As with <0.1 - 268 μg/L (medium value of 30.0 μg/L) in the digestive solution still indicates that workers and children should avoid coming into incidental contact with the soil and ingesting it, especially the high As-bearing soil layers, during the construction and reutilization stage.

ACKNOWLEDGMENTS

The work was supported by the Research Grants Council of the Hong Kong SAR Government (PolyU 5209/11E), the National Basic Research Program of China (973 Program, 2014CB441101), National Natural Science Foundation of China (41603093), and the Civil Engineering and Development Department (CEDD) of the Hong Kong SAR Government (Agreement No. NTE/07/2015). The XAS beam time was granted by beamline BL01C1 and beamline BL16A1 at the National Synchrotron Radiation Research Center, Taiwan. We thank Mr Hao-wei Tu and Mr Shih-Tien Tang for their help in the collection and analysis of spectra. We also thank Dr Wei Zhang from the South China Sea Institute of Oceanology, Chinese Academy of Sciences, for her assistance in the As speciation analysis. We acknowledge the kind help for some XAS spectra, including As(III/ V) adsorption samples on ferrihydrite and goethite from Prof. Chuan-yong Jing (unpublished data performed on beamline X18B at the National Synchrotron Light Source) and Dr. Nabeel Khan Niazi (Niazi et al., 2011, performed on beamline BL-20 at the Australian National Beamline Facility).

Appendix A. Supplementary data

Supplementary data related to this article can be found at https://doi.org/10.1016/j.envpol.2017.09.040.

LIST OF TABLES AND FIGURES

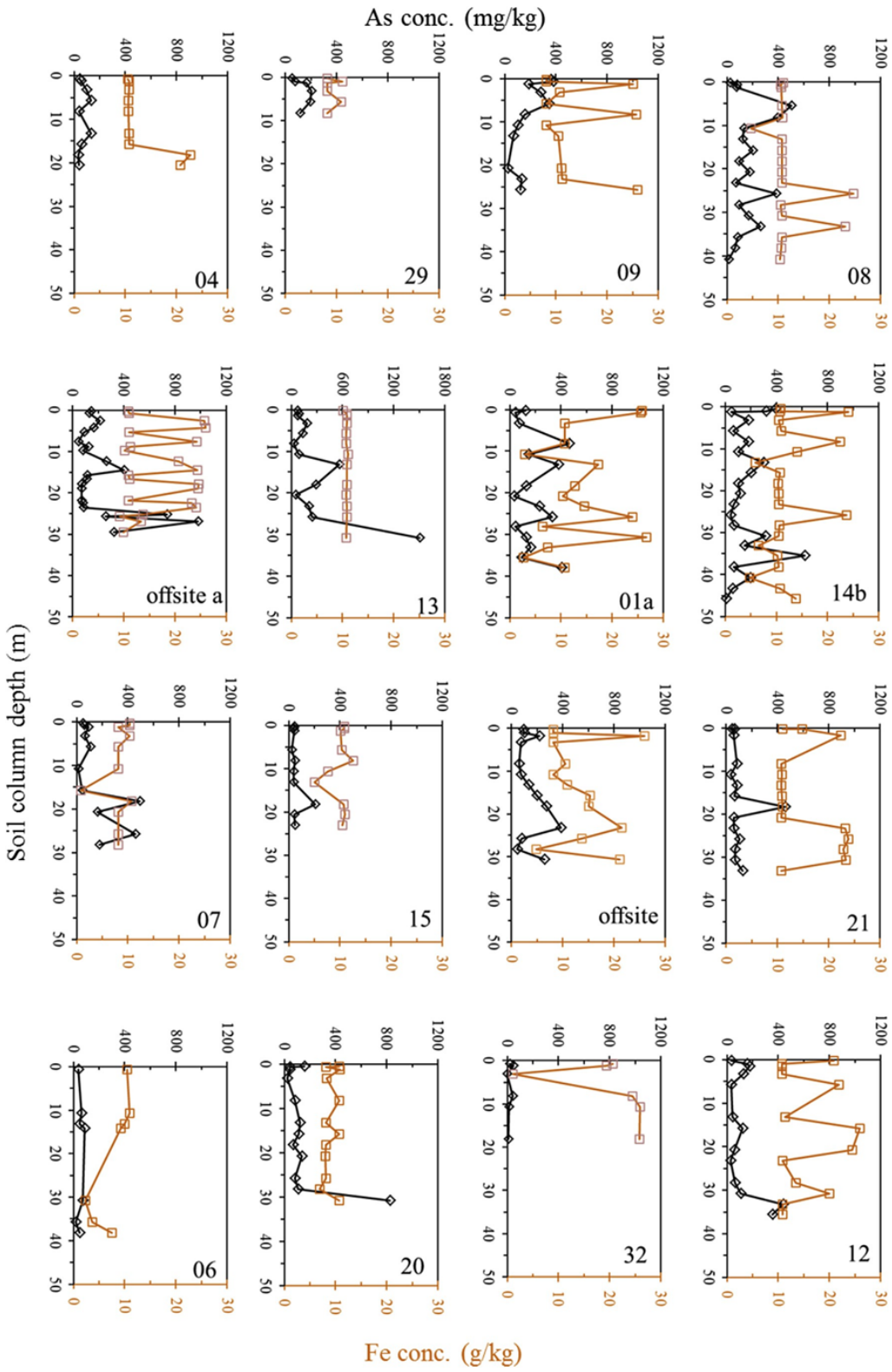

Fig. 1. Depth profiles of As (in black) and Fe (in orange) in soil cores. The label on each panel represents the core number. (For interpretation of the references to colour in this figure legend, the reader is referred to the web version of this article.)

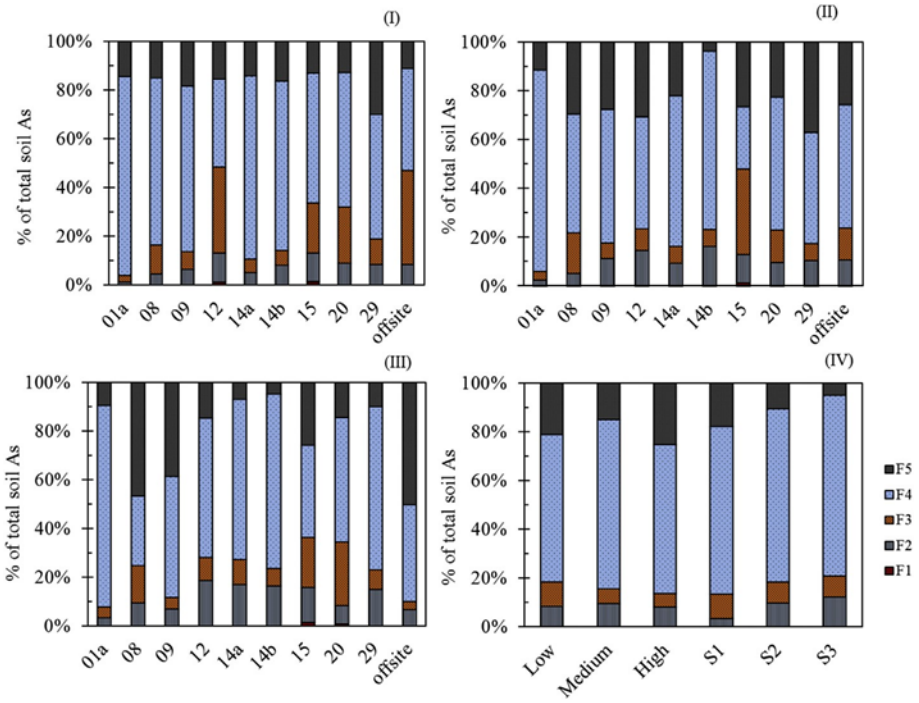

Fig. 2. Sequential extraction fractionations of As in selected soil samples including 0 - 0.5 m (I), 0.5 - 1.0 m (II), 1.0 - 1.5 m (III) from ten soil cores, three blended soil samples (with L representing low As level, M representing a medium As level, and H representing a high As level) (IV) and four deep-layer soil samples (Li et al., 2017) (S1 with 1360 mg-As/kg at 19.2 m from core 3, S2 with 935 mg-As/kg at 25.5 m from core 1, S3 with 304 mg-As/kg at 2.25 m from core 1, and S4 with 227 mg-As/kg at 12.5 m from core 3 (IV)).

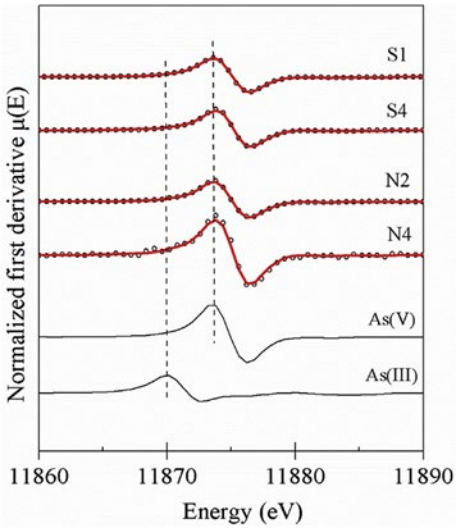

Fig. 3. Characterization of the As valent states of four selected soil samples using first derivative XANES (As K-edge): S1 and S4 with the same information in Fig. 2, N2 with 396 mg-As/kg at 1

m from core 14 b, and N4 with 92.7 mg-As/kg at 0.25 m from the core offsite. XANES data and linear combination fitting (LCF) spectra are shown using black dots and red lines, respectively. Two vertical lines in (I) were marked for As(III) (NaAsO2) and As(V) (Na2HAsO4·7H2O), respectively. Other As standard references can be found in Fig. S2 in the supplementary data. The fitted As species in the four samples are shown in Table S2. (For interpretation of the references to colour in this figure legend, the reader is referred to the web version of this article.)

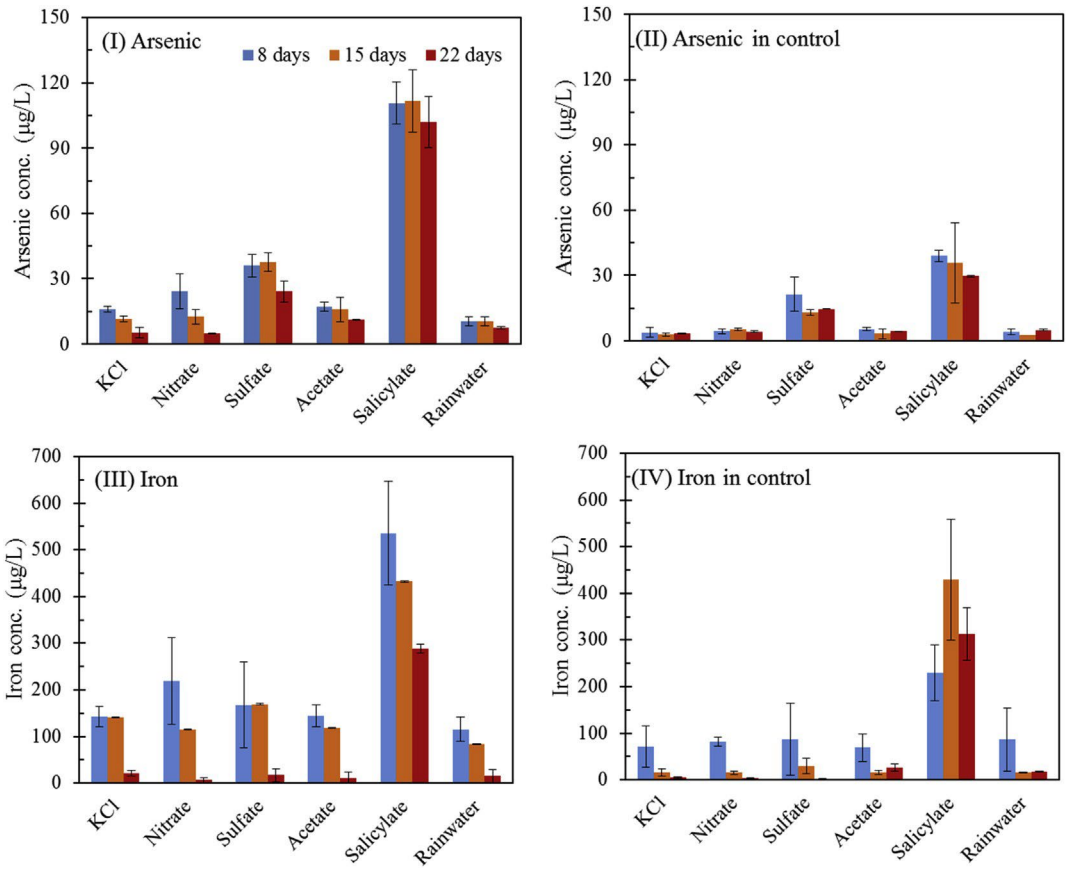

Fig. 4. Arsenic (I-II) and Fe (III-IV) concentrations in suspension under soil incubation with a corresponding sterile control.

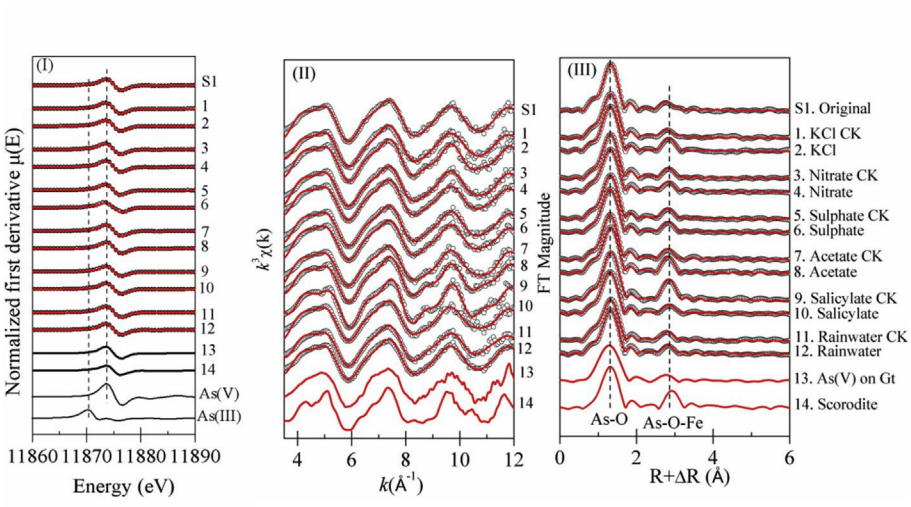

Fig. 5. Arsenic K-edge first derivative XANES analysis by linear combination fitting (LCF) (I); k^3-weighted EXAFS spectra (II) and corresponding Fourier-transform magnitudes (III) (k-range 3-12 $Å^{-1}$) of the original and incubated soil samples by shell-shell fitting. EXAFS data and LCF spectra are depicted using black dots and red lines, respectively. Two vertical lines in (I) were marked for As(III) (NaAsO2) and As(V) (Na2HAsO4$7H2O), respectively. Two standard references are also presented, namely, scorodite (crystalline FeAsO4) and the adsorbed As(V) species on the primary Fe oxide (goethite, Gt, as identified by the Fe K-edge XANES analysis in Fig. S3). The peak positions in panel III were not corrected for the phase shift and they deviated from the true distance by 0.3 - 0.5 Å; detailed information is given in Table 1. (For interpretation of the references to colour in this figure legend, the reader is referred to the web version of this article.)

Table 1
Arsenic K-edge EXAFS fitting results of the original and treated soil.

Sample	As-O			As-*O*-O		As-*O*-Fe			R factor
	CN	R (Å)	σ^2 ($Å^2$)	CN	R (Å)	CN	R (Å)	σ^2 ($Å^2$)	
As(V) on Goethite	4.00 (1)	1.67 (5)	0.004 (1)	12	3.03	1.70 (1)	3.27 (4)	0.002 (0)	0.017
Scorodite	4.23 (1)	1.68 (8)	0.002 (3)	12	3.04	2.92 (3)	3.32 (2)	0.003 (7)	0.012
Original sediment	4.23 (4)	1.69 (0)	0.002 (2)	12	3.04	2.80 (6)	3.22 (2)	0.011 (8)	0.008
KCl	4.27 (2)	1.69 (9)	0.002 (4)	12	3.05	2.01 (6)	3.23 (7)	0.004 (7)	0.010
KCl CK	3.90 (8)	1.69 (7)	0.002 (5)	12	3.05	2.21 (2)	3.21 (2)	0.014 (1)	0.010
Nitrate	4.19 (1)	1.69 (5)	0.002 (8)	12	3.05	2.50 (1)	3.22 (1)	0.008 (0)	0.011
Nitrate CK	4.29 (0)	1.68 (7)	0.002 (3)	12	3.04	2.33 (7)	3.24 (6)	0.007 (6)	0.009
Sulphate	4.38 (7)	1.69 (0)	0.002 (6)	12	3.04	1.67 (8)	3.22 (7)	0.005 (5)	0.011
Sulphate CK	4.27 (2)	1.69 (4)	0.002 (5)	12	3.05	2.24 (2)	3.21 (5)	0.007 (0)	0.008
Acetate	4.17 (7)	1.69 (7)	0.002 (8)	12	3.05	2.31 (6)	3.22 (2)	0.004 (8)	0.008
Acetate CK	4.40 (4)	1.67 (7)	0.002 (3)	12	3.03	1.91 (2)	3.26 (3)	0.006 (2)	0.011
Salicylate	4.69 (3)	1.68 (6)	0.003 (4)	12	3.04	1.74 (2)	3.26 (3)	0.006 (5)	0.012
Salicylate CK	3.91 (5)	1.70 (6)	0.001 (7)	12	3.06	2.81 (6)	3.22 (6)	0.003 (9)	0.012
Rainwater	4.19 (3)	1.69 (4)	0.002 (5)	12	3.05	3.01 (6)	3.22 (2)	0.010 (7)	0.010
Rainwater CK	4.20 (4)	1.70 (6)	0.003 (2)	12	3.06	2.76 (3)	3.19 (1)	0.008 (9)	0.012

CN: coordination number; R(Å): mean half path length; σ^2($Å^2$): Debye-Waller factor; R factor = $\sum i(\text{data}i - \text{fit}i)/\sum i\text{data}$; CN of As-*O*-O multiple path was fixed as 12 multiple scattering paths. The estimated parameter uncertainties for each parameter are listed in parentheses, representing the errors in the last digit; values without reported errors were fixed during fitting.

REFERENCES

Alvarez-Ros, M.C., S'anchez-Corte's, S., García-Ramos, J.V., 2000. Vibrational study of the salicylate interaction with metallic ions and surfaces. Spectrochim. Acta A 56 (12), 2471 - 2477.

Beiyuan, J.Z., Li, J.S., Tsang, D.C.W., Wang, L., Poon, C.S., Li, X.D., Fendrof, S., 2017. Fate of arsenic before and after chemical-enhanced washing of an arsenic- containing soil in Hong Kong. Sci. Total Environ. 599 - 600, 679 - 688.

Bergqvist, C., Herbert, R., Persson, I., Greger, M., 2014. Plants influence on arsenic availability and speciation in the rhizosphere, roots and shoots of three different vegetables. Environ. Pollut. 184, 540 - 546.

Bongoua-Devisme, A.J., Cebron, A., Kassin, K.E., Yoro, G.R., Mustin, C., Berthelin, J., 2013. Microbial communities involved in Fe reduction and mobility during soil organic matter (SOM) mineralization in two contrasted paddy soils. Geo- microbiol. J. 30 (4), 347 - 361.

Burton, E.D., Johnston, S.G., Kocar, B.D., 2014. Arsenic mobility during flooding of contaminated soil: the effect of microbial sulfate reduction. Environ. Sci. Technol. 48 (23), 13660 - 13667.

Chen, N., Jiang, D.T., Cutler, J., Kotzer, T., Jia, Y.F., Demopoulos, G.P., Rowson, J.W., 2009. Structural characterization of poorly-crystalline scorodite, iron(III)e arsenate co-precipitates and uranium mill neutralized raffinate solids using X- ray absorption fine structure spectroscopy. Geochim. Cosmochim. Acta 73 (11), 3260 - 3276.

Chen, T.B., Wong, J.W.C., Zhou, H.Y., Wong, M.H., 1997. Assessment of trace metal distribution and contamination in surface soils of Hong Kong. Environ. Pollut. 96 (1), 61 - 68.

Corsini, A., Cavalca, L., Zaccheo, P., Crippa, L., Andreoni, V., 2011. Influence of microorganisms on arsenic mobilization and speciation in a submerged contam- inated soil: effects of citrate. Appl. Soil Ecol. 49, 99 - 106.

Cui, J.L., Jing, C.Y., Che, D.S., Zhang, J.F., Duan, S.X., 2015a. Groundwater arsenic removal by coagulation using ferric(III) sulfate and polyferric sulfate: a comparative and mechanistic study. J. Environ. Sci. 32 (0), 42 - 53.

Cui, J.L., Du, J.J., Yu, S.W., Jing, C.Y., Chan, T.S., 2015b. Groundwater arsenic removal using granular TiO2: integrated laboratory and field study. Environ. Sci. Pollut. R. 22 (11), 8224 - 8234.

Cui, J.L., Luo, C.L., Tang, C.W.Y., Chan, T.S., Li, X.D., 2017. Speciation and leaching of trace metal contaminants from e-waste contaminated soils. J. Hazard. Mater 329, 150 - 158.

Das, S., Jean, J.S., Kar, S., 2013. Bioaccessibility and health risk assessment of arsenic in arsenic-enriched soils, Central India. Ecotoxicol. Environ. Saf. 92, 252 - 257.

Datta, S., Mailloux, B., Jung, H.B., Hoque, M.A., Stute, M., Ahmed, K.M., Zheng, Y., 2009. Redox trapping of arsenic during groundwater discharge in sediments from the Meghna riverbank in Bangladesh. Proc. Natl. Acad. Sci. U. S. A. 106 (40), 16930 - 16935.

Deng, Y.M., Wang, Y.X., Ma, T., Yang, H., He, J., 2011. Arsenic associations in sedi- ments from shallow aquifers of northwestern Hetao Basin, Inner Mongolia. Environ. Earth Sci. 64 (8), 2001 - 2011.

Eiche, E., Kramar, U., Berg, M., Berner, Z., Norra, S., Neumann, T., 2010. Geochemical changes in individual sediment grains during sequential arsenic extractions. Water Res. 44 (19), 5545 - 5555.

Fendorf, S., Michael, H.A., van Geen, A., 2010. Spatial and temporal variations of groundwater arsenic in South and Southeast Asia. Science 328 (5982), 1123 - 1127.

Fendorf, S., Eick, M.J., Grossl, P., Sparks, D.L., 1997. Arsenate and chromate retention mechanisms on goethite. 1. surface structure. Environ. Sci. Technol. 31 (2), 315 - 320.

Foster, A.L., Kim, C.S., 2014. Arsenic speciation in solids using X-ray absorption spectroscopy. Rev. Mineral. Geochem 79 (1), 257 - 369.

Gr€afe, M., Donner, E., Collins, R.N., Lombi, E., 2014. Speciation of metal(loid)s in environmental samples by X-ray absorption spectroscopy: a critical review. Anal. Chim. Acta 822, 1 - 22.

Guo, H.M., Wen, D.G., Liu, Z.Y., Jia, Y.F., Guo, Q., 2014. A review of high arsenic groundwater in Mainland and Taiwan, China: distribution, characteristics and geochemical processes. Appl. Geochem 41, 196 - 217.

Guo, H.M., Liu, Z.Y., Ding, S.S., Hao, C.B., Xiu, W., Hou, W.G., 2015. Arsenate reduction and mobilization in the presence of indigenous aerobic bacteria obtained from high arsenic aquifers of the Hetao basin, Inner Mongolia. Environ. Pollut. 203, 50 - 59

Haas, J.R., Dichristina, T.J., 2002. Effects of Fe(III) chemical speciation on dissimila- tory Fe(III) reduction by Shewanella putrefaciens. Environ. Sci. Technol. 36 (3), 373 - 380.

Haque, S., Ji, J.F., Johannesson, K.H., 2008. Evaluating mobilization and transport of arsenic in sediments and groundwaters of Aquia aquifer, Maryland, USA. J. Contam. Hydrol. 99 (1 - 4), 68 - 84.

Henke, K.R., 2009. Arsenic: Environmental Chemistry, Health Threats and Waste Treatment. Wiley.

HK CEDD, 2015. Collaboration Research Study on Sustainable Land Decontamination Methods for Application in Land Development Projects (Final Report produced by the research team from the Hong Kong Polytechnic University).

HK EPD, 2007. Guidance Manual for Use of Risk-based Remediation Goals for Contaminated Land Management. Environmental Protection Department.

Hong Kong Observatory, 2011. Meteorological Normals for Hong Kong 1981e2010. Jiang, W., Lv, J., Luo, L., Yang, K., Lin, Y., Hu, F., Zhang, J., Zhang, S., 2013. Arsenate and cadmium co-adsorption and co-precipitation on goethite. J. Hazard. Mater 262, 55 - 63.

Jing, C.Y., Cui, J.L., Huang, Y.Y., Li, A.G., 2012. Fabrication, characterization, and application of a composite adsorbent for simultaneous removal of arsenic and fluoride. ACS Appl. Mater. & Inter 4 (2), 714 - 720.

Johnston, S.G., Diwakar, J., Burton, E.D., 2015. Arsenic solid-phase speciation in an alluvial aquifer system adjacent to the Himalayan forehills. Nepal. Chem. Geol. 419, 55 - 66.

Juhasz, A.L., Smith, E., Weber, J., Rees, M., Rofe, A., Kuchel, T., Sansom, L., Naidu, R., 2007. In vitro assessment of arsenic bioaccessibility in contaminated (anthro- pogenic and geogenic) soils. Chemosphere 69 (1), 69 - 78.

Juhasz, A.L., Weber, J., Smith, E., Naidu, R., Rees, M., Rofe, A., Kuchel, T., Sansom, L., 2009. Assessment of four commonly employed in vitro arsenic bioaccessibility assays for predicting in vivo relative arsenic bioavailability in contaminated soils. Environ. Sci. Technol. 43 (24), 9487 - 9494.

Kelly, S.D., Hesterberg, D., Ravel, B., 2008. Analysis of Soils and Minerals Using X-ray Absorption Spectroscopy. Soil Science Society of America.

Kim, E.J., Yoo, J.C., Baek, K., 2014. Arsenic speciation and bioaccessibility in arsenic-contaminated soils: sequential extraction and mineralogical investigation. En- viron. Pollut. 186, 29 - 35.

Kuhn, K.M., DuBois, J.L., Maurice, P.A., 2013. Strategies of aerobic microbial Fe acquisition from Fe-bearing montmorillonite clay. Geochim. Cosmochim. Acta 117, 191 - 202.

Kuhn, K.M., DuBois, J.L., Maurice, P.A., 2014. Aerobic microbial Fe acquisition from ferrihydrite nanoparticles: effects of crystalline order, siderophores, and alginate. Environ. Sci. Technol. 48 (15), 8664 - 8670.

Li, J.N., Wei, Y., Zhao, L., Zhang, J., Shangguan, Y.X., Li, F.S., Hou, H., 2014. Bio- accessibility of antimony and arsenic in highly polluted soils of the mine area and health risk assessment associated with oral ingestion exposure. Ecotoxicol. Environ. Saf. 110, 308 - 315.

Li, J.S., Beiyuan, J.Z., Tsang, D.C.W., Wang, L., Poon, C.S., Li, X.D., Fendrof, S., 2017. Arsenic-containing soil from geogenic source in Hong Kong: leaching charac- teristics and stabilization/solidification. Chemosphere 182, 31 - 39.

Li, J.Y., Xu, R.K., 2007. Adsorption of phthalic acid and salicylic acid and their effect on exchangeable Al capacity of variable-charge soils. J. Colloid Interface Sci. 306 (1), 3 - 10.

Li, X.D., Lee, S.L., Wong, S.C., Shi, W.Z., Thornton, L., 2004. The study of metal contamination in urban soils of Hong Kong using a GIS-based approach. Envi- ron. Pollut. 129 (1), 113 - 124.

Liu, F., Huang, G.X., Sun, J.C., Jing, J.H., Zhang, Y., 2014. Distribution of arsenic in shallow aquifers of Guangzhou region, China: natural and anthropogenic im- pacts. Water Qual. Res. J. Can. 49 (4), 354 - 371.

Liu, X., Fu, J.W., Guan, D.X., Cao, Y., Luo, J., Rathinasabapathi, B., Chen, Y.S., Ma, L.Q., 2016. Arsenic induced phytate exudation, and promoted FeAsO4 dissolution and plant growth in As-hyperaccumulator Pteris vittata. Environ. Sci. Technol. 50 (17), 9070 - 9077.

Martinez-Lopez, S., Martinez-Sanchez, M.J., Perez-Sirvent, C., Bech, J., Martinez, M.D.G., Garcia-Fernandez, A.J., 2014. Screening of wild plants for use in the phytoremediation of mining-influenced soils containing arsenic in semiarid environments. J. Soils Sed. 14 (4), 794 - 809.

Masscheleyn, P.H., Delaune, R.D., Patrick, W.H., 1991. Effect of redox potential and pH on arsenic speciation and solubility in a contaminated soil. Environ. Sci. Technol. 25 (8), 1414 - 1419.

Meunier, L., Walker, S.R., Wragg, J., Parsons, M.B., Koch, I., Jamieson, H.E., Reimer, K.J., 2010. Effects of soil composition and mineralogy on the bio- accessibility of arsenic from tailings and soil in gold mine districts of Nova Scotia. Environ. Sci. Technol. 44 (7), 2667 - 2674.

Mohapatra, D., Singh, P., Zhang, W., Pullammanappallil, P., 2005. The effect of cit- rate, oxalate, acetate, silicate and phosphate on stability of synthetic arsenic- loaded ferrihydrite and Al-ferrihydrite. J. Hazard. Mater 124 (1e3), 95 - 100.

Ngo, L.K., Pinch, B.M., Bennett, W.W., Teasdale, P.R., Jolley, D.F., 2016. Assessing the uptake of arsenic and antimony from contaminated soil by radish (Raphanus sativus) using DGT and selective extractions. Environ. Pollut. 216, 104 - 114.

Niazi, N.K., Singh, B., Shah, P., 2011. Arsenic speciation and phytoavailability in contaminated soils using a sequential extraction procedure and XANES spec- troscopy. Environ. Sci. Technol. 45 (17), 7135 - 7142.

Niazi, N.K., Burton, E.D., 2016. Arsenic sorption to nanoparticulate mackinawite (FeS): an examination of phosphate competition. Environ. Pollut. 218, 111 - 117.

Ona-Nguema, G., Morin, G., Juillot, F., Calas, G., Brown, G.E., 2005. EXAFS analysis of arsenite adsorption onto two-line ferrihydrite, hematite, goethite, and lepidocrocite. Environ. Sci. Technol. 39 (23), 9147 - 9155.

Pierce, M.L., Moore, C.B., 1982. Adsorption of arsenite and arsenate on amorphous iron hydroxide. Water Res. 16 (7), 1247 - 1253.

Polizzotto, M.L., Harvey, C.F., Sutton, S.R., Fendorf, S., 2005. Processes conducive to the release and transport of arsenic into aquifers of Bangladesh. Proc. Natl. Acad. Sci. U. S. A. 102 (52), 18819 - 18823.

Polizzotto, M.L., Harvey, C.F., Li, G.C., Badruzzman, B., Ali, A., Newville, M., Sutton, S., Fendorf, S., 2006. Solid-phases and desorption processes of arsenic within Bangladesh sediments. Chem. Geol. 228 (1 - 3), 97 - 111.

Raab, A., Williams, P.N., Meharg, A., Feldmann, J., 2007. Uptake and translocation of inorganic and methylated arsenic species by plants. Environ. Chem. 4 (3), 197 - 203.

Root, R.A., Vlassopoulos, D., Rivera, N.A., Rafferty, M.T., Andrews, C., O'Day, P.A., 2009. Speciation and natural attenuation of arsenic and iron in a tidally influ- enced shallow aquifer. Geochim. Cosmochim. Acta 73 (19), 5528 - 5553.

Selim Reza, A.H.M., Jean, J.S., Yang, H.J., Lee, M.K., Woodall, B., Liu, C.C., Lee, J.F., Luo, S.D., 2010. Occurrence of arsenic in core sediments and groundwater in the Chapai-Nawabganj District, northwestern Bangladesh. Water Res. 44 (6), 2021 - 2037.

Sherman, D.M., Randall, S.R., 2003. Surface complexation of arsenic(V) to iron(III) (hydr)oxides: structural mechanism from ab initio molecular geometries and EXAFS spectroscopy. Geochim. Cosmochim. Acta 67 (22), 4223 - 4230.

Smedley, P.L., Kinniburgh, D.G., 2002. A review of the source, behaviour and dis- tribution of arsenic in natural waters. Appl. Geochem 17 (5), 517 - 568.

Tian, H.X., Shi, Q.T., Jing, C.Y., 2015. Arsenic biotransformation in solid waste res- idue: comparison of contributions from bacteria with arsenate and iron reducing pathways. Environ. Sci. Technol. 49 (4), 2140 - 2146.

Tufano, K.J., Fendorf, S., 2008. Confounding impacts of iron reduction on arsenic retention. Environ. Sci. Technol. 42 (13), 4777 - 4783.

van Geen, A., Zheng, Y., Cheng, Z., Aziz, Z., Horneman, A., Dhar, R.K., Mailloux, B.,

Stute, M., Weinman, B., Goodbred, S., Seddique, A.A., Hope, M.A., Ahmed, K.M., 2006. A transect of groundwater and sediment properties in Araihazar, Bangladesh: further evidence of decoupling between as and Fe mobilization. Chem. Geol. 228 (1 - 3), 85 - 96.

Wang, Y., Jiao, J.J., 2014. Multivariate statistical analyses on the enrichment of arsenic with different oxidation states in the Quaternary sediments of the Pearl River Delta, China. J. Geochem. Explor 138, 72 - 80.

Wang, Y., Jiao, J.J., Cherry, J.A., 2012. Occurrence and geochemical behavior of arsenic in a coastal aquifer-aquitard system of the Pearl River Delta, China. Sci. Total Environ. 427, 286 - 297.

Wang, Y., Jiao, J.J., Zhu, S.Y., Li, Y.L., 2013. Arsenic K-edge X-ray absorption near-edge spectroscopy to determine oxidation states of arsenic of a coastal aquifer- aquitard system. Environ. Pollut. 179, 160 - 166.

Watts, H.D., Tribe, L., Kubicki, J.D., 2014. Arsenic adsorption onto minerals: con- necting experimental observations with density functional theory calculations. Minerals 4 (2), 208e240.

Wenzel, W.W., Kirchbaumer, N., Prohaska, T., Stingeder, G., Lombi, E., Adriano, D.C., 2001. Arsenic fractionation in soils using an improved sequential extraction procedure. Anal. Chim. Acta 436 (2), 309 - 323.

Youngran, J., Fan, M.H., Van Leeuwen, J., Belczyk, J.F., 2007. Effect of competing solutes on arsenic(V) adsorption using iron and aluminum oxides. J. Environ. Sci. 19 (8), 910 - 919.

Zhang, H.H., Yuan, H.X., Hu, Y.G., Wu, Z.F., Zhu, L.A., Zhu, L., Li, F.B., Li, D.Q., 2006.

Spatial distribution and vertical variation of arsenic in Guangdong soil profiles, China. Environ. Pollut 144 (2), 492 - 499.

Zhang, W., Wang, W.X., Zhang, L., 2013. Arsenic speciation and spatial and inter- species differences of metal concentrations in mollusks and crustaceans from a South China estuary. Ecotoxicology 22 (4), 671 - 682.